A Single ZnO Nanofiber-Based Highly Sensitive Amperometric Glucose Biosensor

Mashkoor Ahmad, Caofeng Pan, Zhixiang Luo, and Jing Zhu*

Beijing National Center for Electron Microscopy, The State Key Laboratory of New Ceramics and Fine Processing, Laboratory of Advanced Material, China Iron & Steel Research Institute Group, Department of Material Science and Engineering, Tsinghua University, Beijing 100084, China

Received: March 19, 2010; Revised Manuscript Received: April 17, 2010

A novel fabrication approach of a highly sensitive amperometric glucose biosensor based on a single ZnO nanofiber (ZONF) is presented. Nanofibers (NFs) of poly(vinyl pyrrolidone)/zinc acetate composite have been synthesized by electrospinning technique. By high-temperature calcinations of the above precursor fibers, ZONFs with diameters in the range of 350−195 nm have been successfully obtained. A single NF on a gold electrode is functionalized with glucose oxidase (GOx) by physical adsorption. Electrochemical measurements of the biosensor revealed a high and reproducible sensitivity of 70.2 μA cm^{-2} mM^{-1} within a response time of less than 4 s. The biosensor also showed a linear range from 0.25 to 19 mM with a low limit of detection (LOD) of 1 μM. Furthermore, it has been revealed that the biosensor exhibits a good anti-interference ability and favorable stability over relatively long-term storage (more than 4 months). All these results strongly suggest that a single ZONF can provide a new platform for biosensor design and other biological applications.

I. Introduction

The unique and fascinating properties of nanostructured materials have triggered tremendous motivation among scientists to explore the possibilities of using them in industrial and medical applications. Biosensors are becoming essential in the fields of health care, chemical and biological analysis, environmental monitoring, and good processing industries.[1,2] Among them, glucose sensors, as one of the most popular biosensors, have been extensively investigated due to their important clinical applications. The fast and accurate determination of glucose has profound applications, since glucose concentration is a crucial indicator in many diseases, such as diabetes and endocrine metabolic disorder. In recent years, many efforts have been made to develop reliable glucose biosensors using electrochemical methods,[3] chemiluminescence,[4] or other methods.[5] Among all the methods, the enzyme-involved electrochemical glucose biosensor has been widely studied because of its simplicity, high selectivity and relative low cost.[6−8] Among the numerous reports in glucose biosensors, the immobilization of enzymes on a suitable matrix and their stability are important factors in the fabrication of the biosensors.[9] The immobilization of glucose oxidase (GOx), a widely used analytical enzyme for glucose detection, has been realized by various methods, such as physical adsorption, cross-linking, self-assembly, incorporation in carbon paste, polymers, and sol−gels, etc.[10−15]

On the other hand, nanostructures have unique advantages in immobilization enzymes and can retain their bioactivity as a result of the high surface area for higher enzyme loading, desirable microenvironment, and the direct electron transfer between the enzyme's active sites and the electrode.[16−19] Glucose biosensors, making use of a titania sol−gel membrane, carbon nanotubes, Au nanoparticles, TiO_2 nanoporous film, and ZrO_2/chitasan composite film to immobilize enzymes, have been reported.[15,20−22] Recently, ZnO and its one-dimensional (ID) nanostructures have been investigated intensively due to their potential in optoelectronics and biomedical applications. On the other hand, ZnO nanostructures present as one of the most promising materials for the fabrication of efficient amperometric biosensors due to having exotic and versatile properties including biocompatibility, nontoxicity, chemical and photochemical stability, high specific surface area, optical transparency, electrochemical activities, high electron communicating features, and so on.[23−25] As ZnO has a high isoelectric point (IEP) of about 9.5, it is suitable for adsorption of a low IEP protein or enzyme such as GOx (IEP $\sim$ 4.2) in proper buffer solutions.[26] ZnO nanostructures have been synthesized by various techniques using arc discharge, laser vaporization, pyrolysis, electrodeposition, physical vapor deposition, and chemical vapor deposition.[27−30]

Furthermore, for a large-scale production of micro- and nanofibers (NFs) of organic polymers, composites, and inorganic oxide materials, electrospinning is known as the most effective technique and has the advantages of low cost and easy preparation without any limitation of size.[31,32] The as-spun NFs can be directly collected as either nanowoven mats or uniaxially aligned arrays, and already have applications that include reinforcement of composite materials, ultrafiltration, tissue engineering, catalysis, as well as the fabrication of sensors, batteries, and other types of devices.[33−37] Due to their large specific surface area, NFs are expected to efficiently enhance the performance of a biosensor. Although glucose biosensors based on ZnO nanostructures such as nanowires, nanotubes, nanocombs, and nanorods have been already reported,[38−41] a single ZnO nanofiber (ZONF)-based glucose biosensor has not been reported yet. As it is well-known that the performance of a biosensor heavily relies on the supporting materials, in searching for suitable material in the present work, ZONFs were synthesized by using the electrospinning technique. As a simple fabrication approach, a single ZONF-based amperometric glucose biosensor was fabricated that shows high sensitivity.

II. Experimental Section

II.1. Materials and Apparatus. GOx (EC 1.1.3.4 from *Aspergillus niger*, 100 U/mg) and poly(vinyl pyrrolidone) (PVP;

* Crossponding author E-mail: Jzhu@mail.tsinghua.edu.cn, Fax: 86-10-62771160.

10.1021/jp102505g
Published on Web 05/03/2010

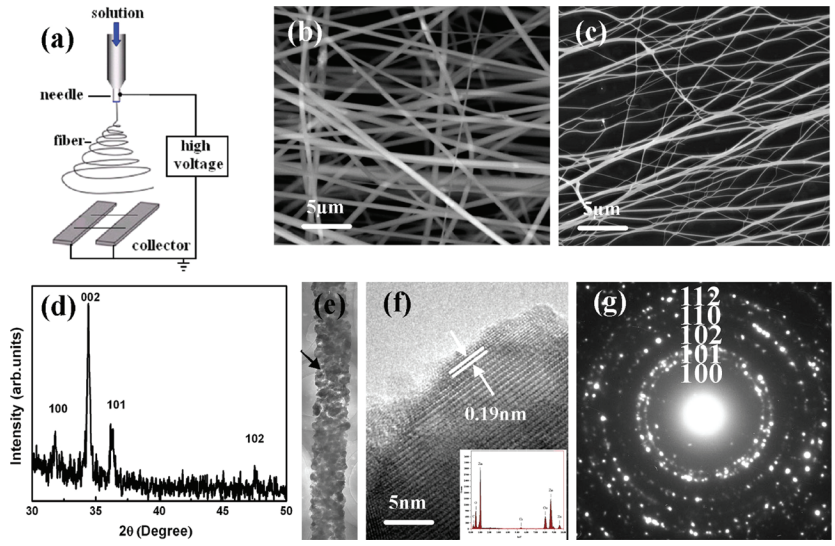

Figure 1. (a) Schematic of electrospinning experimental setup used for the fabrication of ZONFs. (b) SEM image of the as-prepared NF. (c) SEM image of the NF after calcinations at 700 °C for 5 h. (d) XRD pattern of the ZONF after calcinations at 700 °C for 5 h. (e) TEM image of an individual ZONF. (f) Bright field HRTEM image of the NF; inset is the corresponding EDS of the NF. (g) Corresponding SAED of the NF.

MW ~ 1 300 000) were purchased from Sigma-Aldrich. Glucose, cholesterol, L-cysteine (L-Cys), ascorbic acid (AA), urea, and citric acid were purchased from Sinopharm Chemical Regent Co., Ltd. Other chemicals were of analytical-regent grade without further purification. The pH of 0.1 M phosphate buffer (PB) solution was adjusted by HNO_3 and NaOH. Glucose stock solution was kept for at least 24 h after preparation for mutarotation. All solutions in the testing were prepared using deionized water. The electrochemical experiments were performed at room temperature utilizing an electrochemical workstation (CHI660C) with a three-electrode mode: the modified gold electrode was used as the working electrode, with Hg/Hg_2SO_4 as the reference electrode, and silver as the counter electrode. The pH of the solution was measured in real time by a pH meter. The as-synthesized NFs were characterized by a scanning electron microscope (SEM-6301F), X-ray diffraction (XRD), a high-resolution transmission electron microscope HRTEM (JEM-2011), and a Keithley 2400 sourcemeter.

II.2. Synthesis of NFs through Electrospinning. Electrospinning provided a simple and versatile method for producing polymer fibers. A precursor polymer solution was prepared containing 0.5 g of 10% zinc acetate (99.0%) and 0.26 g of PVP in 0.7 g of ethanol. In a typical procedure, the precursor polymer solution was loaded into a plastic syringe equipped with a stainless-steel needle, and the distance between the needle tip and the collector was 10 cm. The needle was connected to a high-voltage power supply (operated at 15 kV) during electrospinning, after which the zinc acetate/PVP solutions were electrospun. The solution ejected from the tip of the needle travels through the air to its target medium and accumulates as a nonwoven fiber mat. The collector used here was composed of two conductive substrates separated by a void gap as shown in Figure 1a. Then the as-synthesized NFs were transferred onto the as-prepared cleaned silicon substrate. By high-temperature calcinations of the above precursor fibers, ZONFs were successfully obtained.

II.3. Fabrication of Single-NF-Based Glucose Biosensor. To fabricate the biosensor, the as-prepared individual ZONF after calcinations at 700 °C is transferred to a conventional gold electrode (with 3 mm diameter) under a high-resolution microscope. The as-prepared ZONF/gold electrode is then wetted by PB solution and dried in air for 2 h. A 5 μL portion of 0.25% poly(vinyl alcohol) (PVA) solution is dropped onto the ZONF/gold electrode and dried to form a film on the individual NF, which is critical to attach the ZONF tightly on the surface of the gold electrode. Following the evaporation of water, a 5 μL GOx solution along with 5 μL of 0.01 mol/L L-Cys is dropped onto the surface of the ZONF/gold electrode via physical adsorption. The modified electrode (L-Cys/GOx/PVA/ZONF/gold electrode) is kept at 4 °C in a refrigerator overnight followed by an extensive washing step to remove the immobilized GOx.

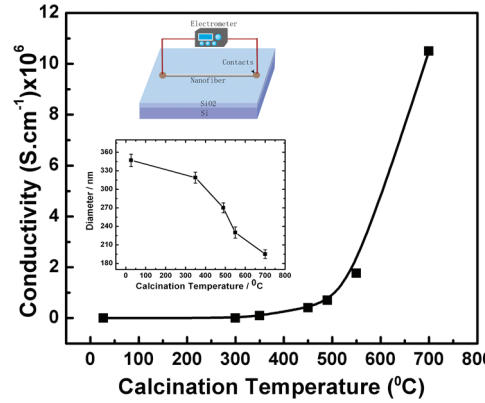

Figure 2. Conductivity of the individual ZONFs after different calcination temperatures. Inset: diameter vs calcination temperature and optical microscope image of an individual NF.

III. Results and Discussion

III.1. NF Characterization. Figure 1b shows the SEM image of the as-prepared NFs of PVP/ZnO. It can be seen that the fibers aligned in random orientation because of the bending instability associated with the spinning jet. The average diameter of the as-prepared fibers is about 350 nm, and the length can even reach millimeter grade. The diameter of the fibers is obtained (~195 nm) after calcinations at 700 °C, as shown in Figure 1c. The structure and phase purity of the NFs are characterized by an XRD pattern, as shown in Figure 1d. It has been seen from the pattern that all major diffraction peaks correspond to the ZnO crystal faces. The evaluated *c*-axis lattice constant of the NF is 0.5140 nm, which is same as that of the

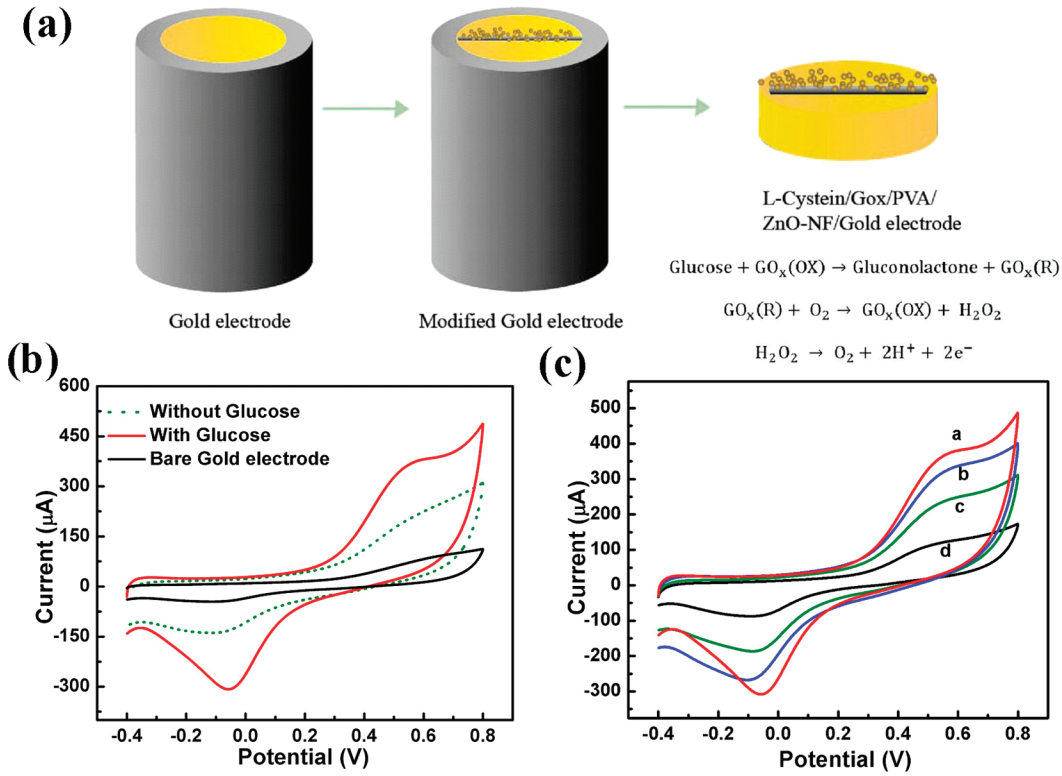

Figure 3. (a) Schematic diagram of the modified gold electrode and the mechanism of the glucose sensing on the modified electrode. (b) Cyclic voltammograms of the bare and modified gold electrode without and with 100 μM glucose in pH 7.0 PB solution. (c) Cyclic voltammograms of the biosensor in PB solution (pH 7.0) containing 100 μM glucose at a scan rate of (a) 100 mV, (b) 80, (c) 50, and (d) 20 mV s^{-1}.

ZnO (c = 0.5109 nm). Figure 1e shows the TEM image of the individual ZONF. It can be seen from the picture that the fiber could be very useful for enzyme loading due to havinga large surface area and porous structure. The HRTEM image shows the polycrystalline nature of the fiber, and the spacing distances between two adjacent fringes in different planes are calculated as shown in Figure 1f. These spacing distances are also consistent with the lattice constant of bulk ZnO (JCPDS Card No. 80-0075). The inset in Figure 1f shows the corresponding in situ energy-dispersive X-ray spectroscopy (EDS) elemental analysis of the NF. An oxygen peak at about 0.52 KeV and Zn peaks at about 1.02, 8.67, and 9.60 KeV can be observed in the spectrum. The signals of Cu, C, and Cr peaks come from the surface of the copper grid used for TEM measurements. The corresponding selected area electron diffraction (SAED) pattern is recorded as shown in Figure 1g. The lattice constants calculated from the SAED are 3.2552 Å for a and 5.2113 Å for c, which are also consistent with those of ZnO (a = 3.2535 Å, c = 5.2151 Å). These results are also good agreement with XRD.

III.2. Conductivity Measurements of the NF. In order to investigate the electrical properties of the fiber, I−V measurements have been performed using a Keithley 2400 sourcemeter. In this experiment, an NF after each calcination temperature is placed on the Si substrate having a 600 nm SiO_2 layer, and contacts are made with silver paste to the ends of the fiber keeping constant length as shown in Figure 2 (inset). Copper wires are connected to these contacts for I−V measurements. The conductivity (σ) of the NF as a function of the calcination temperature is calculated using their corresponding resistance R, length L, and cross sectional area as $\sigma = L/RA$. Figure 2 shows the calculated conductivity versus calcinations plot for the individual NF. It shows how the conductivity of the fiber changes with the increase of calcination temperature. The maximum conductivity of 10.5 × 10^6 S·cm^{-1} is achieved after calcinations at 700 °C, as shown in the figure. It illustrates that the decrease in diameter by increasing the calcination temperature (see inset in the figure) leads to reduction of the cross-sectional area of the fiber, which results in an increase in conductivity.

III.3. Biosensor Electrochemical Measurements. Figure 3a schematically illustrates the mechanism of the process, in which glucose would be oxided by GOx(OX) to gluconolactone, while GOx(OX) is changed into the reductive form GOx(R). The consumed GOx(OX) could be regenerated from GOx(R) through its reaction with the oxygen present in solution. This process produces H_2O_2, which can be detected quantitatively on the modified electrode. Figure 3b shows cyclic voltammetric (CV) sweep curves for the bare (black line) and ZONF-modified gold electrode without glucose (dotted line) and with 100 μM glucose (red line) at the scan rate of 100 mVs^{-1} in the range of −0.4 to 0.8 V. It can be seen that, in contrast to the bare and modified electrode without glucose, the oxidation current increases significantly, which relates to the oxidation of glucose by GOx catalysis. Moreover, in contrast to the reduction peak at around −0.05 V, a strong oxidation peak is also observed with peak potential at +0.54 V, which can be ascribed to H_2O_2 generated during the oxidation of glucose as reported.[42] Figure 3c shows the plot of CV profiles obtained at different scan rates and demonstrates a linear increase in the oxidation and reduction peak currents. It can be found that the peak current is proportional to the square root of the scan rate, showing a typical diffusion-controlled electrochemical behavior.

III.4. Performance of the Biosensor. ***III.4.1. Calibration Curve and Detection Limit.*** The performance of the biosensor has been investigated under different tests. Figure 4a shows the amperometric response of the modified electrode on the successive addition of glucose (from 1 μM to 20 mM) into

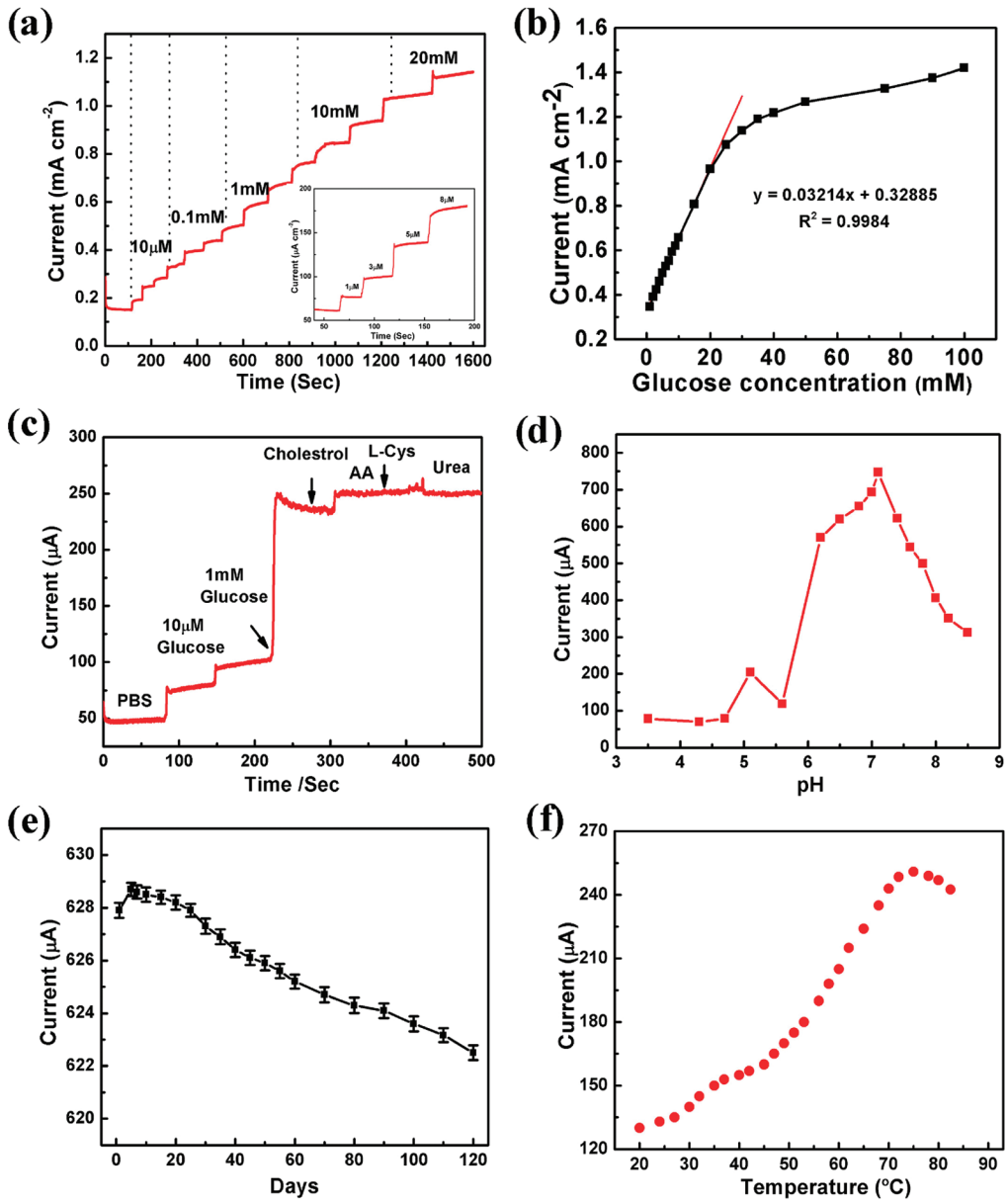

Figure 4. (a) Amperometric response of the biosensor based on ZONF to different concentrations of glucose at 0.8 V in a stirring pH 7.0 PB solution. Inset (bottom right): Response of biosensor with successive addition of glucose showed low LOD. (b) Calibrated curve of the biosensor with successive addition of glucose. (c) Effect of interfering species to the response of the biosensor. (d) Amperometric response of the ZONF-based glucose biosensor in PB solution with increasing pH containing 0.1 mM glucose. (e) Long-term stability of the biosensor. (f) Temperature profile of the biosensor in PB solution with 10 μM glucose.

continuously stirred 0.1 M PB solution (pH = 7.0) at an applied potential +0.8 V. It has been revealed that the biosensor exhibits a rapid and sensitive response to the change of glucose concentration and an obvious increase in current upon successive addition of glucose. The modified electrode achieved 95% steady-state current within less than 4 s. This indicates a good electrocatalytic oxidative and fast electron exchange behavior of the ZONF-modified electrode. The corresponding calibration curve of the biosensor is shown in Figure 4b. Following the increase of the glucose concentration, the response current increases and saturates at a high glucose concentration of about 50 mM. The linear range of the calibration curve is from 0.25 mM to 19 mM (correction coefficient $R = 0.9984$) with a low limit of detection (LOD) of about 1 μM (inset bottom right, Figure 4a). The sensitivity of the biosensor is about 70.2 μA cm^{-2} mM^{-1}, which is much higher than that of the other ZnO nanostructure-based biosensors,[38−41] due to the large specific surface area for higher enzyme loading, enhanced electrostatic interaction, and providing a compatible microenvironment to help the enzyme to retain its bioactivity of the NF. To the best of our knowledge, this is the first time such a high sensitivity has been achieved for a glucose biosensor by using an L-Cys/GOx/PVA/ZONF/glassy carbon electrode (GCE)-modified electrode. These results prove that ZONFs used as a matrix provide a good environment for the enzyme activity to enhance the sensitivity of the modified electrode to glucose detection.

III.4.2. Michaelis−Menten Constant (K_m). The apparent Michaelis−Menten constant (K_m) is used to evaluate the biological activity of the immobilized enzyme, and it can be calculated by using the Lineweaver−Burk equation $1/i_s = (k_m/i_{max})(1/C_g) + 1/i_{max}$, where i_s is the steady state current, C_g is the glucose concentration, K_m is the apparent Michaelis−Menten constant, and i_{max} is the maximum current. From the i_s^{-1} versus C_g^{-1} curve, based on the experimental data from Figure 4b, the

TABLE 1: Comparison of the Performance Parameters of Glucose Biosensor Based on Single ZONF with Other ZnO Nanostructures

electrode materials	sensitivity/ μA mM^{-1} cm^{-2}	linear range/mM	response time/s	appl. potential (V)	detection limit (μM)	ref.
ZnO/MWNTs	50	0.1−16		0.4	0.25	29
ZnO nanocombs	15.33		<10	0.8	20	31
ZnO nanorods	23.1	0.01−3.45	<5	0.8	10	27
ZnO nanodisks	16.9		<10	0.6	10	31
ZnO nanotubes	30.85	0.01−4.2	<6	0.8	10	30
ZnO/PVP NF	70.2	0.25−19	<4	0.8	1.0	present work

K_m is estimated to be 2.19 mM. The small K_m means that the immobilized GOx possesses a high enzymatic activity, and the proposed electrode exhibits a high affinity for glucose.[43]

III.4.3. Anti-interferences. It is well known that some electroactive species in serum may influence the performance of a biosensor; therefore, the anti-interference ability of the biosensor is investigated by introducing electroactive species such as cholesterol, AA, L-Cys, and urea. These species are consecutively added into a continuously stirred 0.1 M PB solution at an applied potential of +0.8 V with a scan rate of 0.1 V s^{-1}. The influence of cholesterol, AA, L-Cys, and urea on the detection of glucose at the modified electrode is shown in Figure 4c. It is observed that the cholesterol and L-Cys do not have any obvious effect on the biosensor, while AA can cause a small current increment of about 10% compared with the 1 mM glucose. However, an increase in current of about 3% is also observed when 0.5 M urea is added. Considering that the concentration of AA in physiological conditions is below 0.5 mM (around 0.1 mM)[44] and much smaller than that of glucose, it also has a negligible effect on the glucose detection in the serum sample. These results indicate that the proposed glucose biosensor exhibits the ability to reduce the influence of possible interferences. All the above results demonstrate that the constructed biosensor has a good anti-interference ability.

III.4.4. pH Effect. The activity of the enzyme GOx is heavily affected by the pH of the glucose solution; therefore, the pH effect on the biosensor performance is also investigated by measuring the current response to 0.1 mM glucose at +0.8 V. As ZnO is a kind of amphoteric compound and not stable in both strong acid and base solutions, the pH dependence of the biosensor is evaluated in the range of pH 3.5−8.5 in this experiment. As clearly seen in Figure 4d, the biosensor shows an optimal sensitivity of response at pH 7.1, corresponding to a series of pH values. Considering that the pH of human blood is about 7.4, all the amperometric experiments have been carried out at pH 7.0.

III.4.5. Long-Term Stability. The long-term stability of the biosensor is also evaluated by measuring its performance every few days, as shown in Figure 4e. It can be seen that the biosensor shows high stability for glucose detection, which retains about 95% of its original response to glucose after 120 days of storage. The small decrease in glucose response may be due to the loss of the bioactivity of the immobilized GOx with the passage of time.

III.4.6. Thermal Stability of the Biosensor. Enzymes or proteins are susceptible to thermal denaturation; however, when they are immobilized onto the conducting surface, their thermal behavior will differ from that when they are in the "free" state.[45] The thermal stability of the biosensor has been examined by measuring the response of the biosensor with 10 μM glucose between 20 and 85 °C, as shown in Figure 4f. It has been revealed that the biosensor response gradually increases with increasing temperature and reaches its optimum value at 75 °C. This is because of the increases in enzyme activity at higher temperature. After optimum temperature, the response decreases, which is caused by the natural degradation of the enzyme. The excellent thermoresistance of the biosensor is ascribed to the ZONF film. The hydrophobic ZONF provides a favorable environment for the immobilized GOx, which greatly enhances the thermal stability of the biosensor. This suggests that the biosensor could be used in an environment within a temperature range of 20−85 °C. All other operation is done at room temperature.

III.4.7. Performance Comparison. The characteristics and performance of the fabricated biosensor is compared with the previously reported glucose biosensors based on the utilization of various ZnO nanostructures as the working electrode as shown in the Table 1. It is confirmed that the presented glucose biosensor exhibited an excellent performance.

IV. Conclusions

In conclusion, a highly sensitive glucose biosensor based on a single ZONF has been successfully fabricated and revealed that the ZONF improved the electrocatalytic activity of the enzyme, which in turn enhanced the sensitivity of the biosensor for glucose detection. Furthermore, the performance of the biosensor showed high and reproducible sensitivity of 70.2 μA mM^{-1} cm^{-2} with a response time of less than 4 s and a linear range from 0.25 to 19 mM. It also exhibits good anti-interference ability and favorable stability over relatively long-term storage (more than 4 months). To the best of our knowledge, this is the first time such a highly sensitive glucose biosensor has been achieved by using an L-Cys/GOx/PVA/ZONF/gold-modified electrode. The large surface area, together with the good electrical properties, made the NFs promising materials for sensing applications. This study would probably provide an economic way to meet the industrial requirements of a low-cost processing technique for large-scale production.

Acknowledgment. This work is financially supported by the National 973 Project of China and Chinese National Nature Science Foundation. The authors also thank the Higher Education Commission (HEC) and PINSTECH (PAEC) of Pakistan for the financial support to Mashkoor Ahmad.

References and Notes

(1) Rakow, N. A.; Suslick, K. S. *Nature (London)* **2000**, *406*, 710.
(2) Ahmad, M.; Pan, C.; Gan, L.; Zeeshan, N; Zhu, J. *J. Phys. Chem. C* **2010**, *114*, 243.
(3) Ye, J. S.; Wen, Y.; Zhang, W. D.; Gan, L. M.; Xu, G. Q.; Sheu, F. S. *Electrochem. Commun.* **2004**, *6*, 66.
(4) Zhu, L.; Li, Y.; Tian, F.; Xu, B.; Zhu, G. *Sens. Actuators, B: Chem.* **2002**, *84*, 265.
(5) Shafer-Peltier, K. E.; Haynes, C. L.; Glucksberg, M. R.; Van Duyne, R. P. *J. Am. Chem. Soc.* **2003**, *125*, 588.
(6) Lee, D.; Lee, J.; Kim, J.; Na, H. B.; Kim, B.; Shin, C. H.; Kwak, J. H.; Dohnalkova, A.; Grate, J. W.; Hyeon, T.; Kim, H. S. *Adv. Mater.* **2005**, *17*, 2828.
(7) Luo, X. L.; Xu, J. J.; Du, Y.; Chen, H. Y. *Anal. Biochem.* **2004**, *334*, 284.

(8) Zhao, W.; Xu, J. J.; Shi, C. G.; Chen, H. Y. *Langmuir* **2005**, *21*, 9630.
(9) Shen, J.; Liu, C. C. *Sens. Actuators, B: Chem.* **2007**, *120*, 417.
(10) Battaglini, F.; Bartlett, P. N.; Wang, J. H. *Anal. Chem.* **2000**, *72*, 502.
(11) Burmeister, J. J.; Gerhardt, G. A. *Anal. Chem.* **2001**, *73*, 1037.
(12) Murthy, A. S. N.; Sharma, J. *Anal. Chim. Acta* **1998**, *363*, 215.
(13) Kulys, J.; Tetianec, L.; Schneider, P. *Biosens. Bioelectron.* **2001**, *16*, 319.
(14) Palmisano, F.; Rizzi, R.; Entonze, D.; Zambonin, P. G. *Biosens. Bioelectron.* **2000**, *15*, 531.
(15) Yu, J. H.; Liu, S. Q.; Ju, H. X. *Biosens. Bioelectron.* **2003**, *19*, 401.
(16) Yadav, H. K.; Gupta, V.; Sreenivas, K.; Singh, S. P.; Sundarakannan, B.; Katiyar, R. S. *Phys. Rev. Lett.* **2006**, *97*, 085502.
(17) Xiao, Y.; Patolsky, F.; Katz, E.; Hainfeld, F.; Willner, I. *Science* **2003**, *299*, 1877.
(18) Jia, J.; Wang, B.; Wu, A.; Cheng, G.; Li, Z.; Dong, S. A. *Anal. Chem.* **2002**, *74*, 2217.
(19) Xu, Q.; Mao, C.; Liu, N. N.; Zhu, J. J.; Sheng, J. *Biosens. Bioelectron.* **2006**, *22*, 768.
(20) Hrapovic, S.; Liu, Y. L.; Male, K. B.; Luong, J. H. T. *Anal. Chem.* **2004**, *76*, 1083.
(21) Yang, Y. H.; Yang, H. F.; Yang, M. H.; Liu, Y. L.; Shen, G. L.; Yu, R. Q. *Anal. Chim. Acta* **2004**, *525*, 213.
(22) Chara, T. J.; Rajagopalan, R.; Heller, A. *Anal. Chem.* **1999**, *466*, 2451.
(23) Ahmad, M.; Pan, C.; Iqbal, J.; Gan, L.; Zhu, J. *Chem. Phys. Lett.* **2009**, *480*, 105.
(24) Kang, B. S.; Ren, F. Y.; Heo, W.; Tien, L. C.; Norton, D. P.; Pearton, S. J. *Appl. Phys. Lett.* **2005**, *86*, 112105.
(25) Zhang, F.; Wang, X.; Ai, S.; Sun, Z.; Wan, Q.; Zhu, Z.; Xian, Y.; Jin, L.; Yamamoto, K. *Anal. Chim. Acta* **2004**, *519*, 155.
(26) Topoglidis, E.; Cass, E. G.; O'Regan, B.; Durrant, J. R. *Electroanal. J. Chem.* **2001**, *517*, 20.
(27) Han, W. Q.; Fan, S. S.; Li, Q. Q.; Hu, Y. D. *Science* **1997**, *277*, 1287.
(28) Ahmad, M.; Zhao, J.; Iqbal, J.; Miao, W.; Xie, L.; Mo, R.; Zhu, J. *J. Phys. D: Appl. Phys.* **2009**, *42*, 165406.
(29) Li, Y.; Meng, G. W.; Zhang, L. D.; Phillipp, F. *Appl. Phys. Lett.* **2000**, *76*, 2011.
(30) Kun, Y.; Guang, W. S.; Hui, W.; Xue, M. O.; Xiao, H. Z.; Chun, S. L.; Shuit, T. L. *J. Phys. Chem. C* **2009**, *113*, 20169.
(31) Reneker, D. H.; Chun, I. *Nanotechnology* **1996**, *7*, 216.
(32) Li, D.; Xia, Y. *Adv. Mater.* **2004**, *16*, 1151.
(33) Bergshoef, M. M.; Vancso, G. J. *Adv. Mater.* **1999**, *11*, 1362.
(34) Li, W. J.; Laurencin, C. T.; Caterson, E. J.; Tuan, R. S.; Ko, F. K.; Biomed, *J. Mater. Res.* **2002**, *60*, 613.
(35) Jia, H.; Zhu, G.; Vugrinovich, B.; Kataphinan, W.; Reneker, D. H.; Wang, P. *Biotechnol. Prog.* **2002**, *18*, 1027.
(36) Wang, X.; Drew, C.; Lee, S. H.; Senecal, K. J.; Kumar, J.; Samuelson, L. A. *Nano Lett.* **2002**, *2*, 1273.
(37) Kim, C.; Yang, K. S. *Appl. Phys. Lett.* **2003**, *83*, 1216.
(38) Wei, A.; Sun, X. W.; Wang, J. X.; Lei, Y.; Cai, X. P.; Li, C. M.; Dong, Z. L.; Huang, W. *Appl. Phys. Lett.* **2006**, *89*, 123902.
(39) Wang, Y. T.; Yu, L.; Zhu, Z. Q.; Zhang, J.; Zhu, J. Z.; Fan, C. *Sens. Actuators, B: Chem.* **2009**, *136*, 332.
(40) Kong, T.; Chen, Y.; Ye, Y.; Zhang, K.; Wang, Z.; Wang, X. *Sens. Actuators, B: Chem.* [Online early access]. DOI: 10.1016/j.snb.2009.01.002.
(41) Sun, X. W.; Wang, J. X.; Wei, A. *J. Mater. Sci. Technol.* **2008**, *24*, 649.
(42) Wang, J. X.; Sun, X. W.; Wei, A.; Lei, Y.; Cai, X. P.; Li, C. M.; Dong, Z. L. *Appl. Phys. Lett.* **2006**, *88*, 233106.
(43) Wang, B.; Li, B.; Deng, Q.; Dong, S. *Anal. Chem.* **1998**, *70*, 3170.
(44) Zhao, Z. X.; Qiao, M. Q.; Yin, F.; Shao, B.; Wu, B. Y.; Wang, Y. Y.; Wang, X. S.; Qin, X.; Li, S.; Yu, L.; Chen, Q. *Biosens. Bioelectron.* **2007**, *22*, 3021.
(45) Weetall, H. H. *Anal. Chem.* **1974**, *46*, 602A.

JP102505G